Cell Reports, Volume *42*

Supplemental information

Architecture of androgen receptor pathways amplifying glucagon-like peptide-1 insulinotropic action in male pancreatic β cells

Weiwei Xu, M.M. Fahd Qadir, Daniela Nasteska, Paula Mota de Sa, Caroline M. Gorvin, Manuel Blandino-Rosano, Charles R. Evans, Thuong Ho, Evgeniy Potapenko, Rajakrishnan Veluthakal, Fiona B. Ashford, Stavroula Bitsi, Jia Fan, Manika Bhondeley, Kejing Song, Venkata N. Sure, Siva S.V.P. Sakamuri, Lina Schiffer, Wandy Beatty, Rachael Wyatt, Daniel E. Frigo, Xiaowen Liu, Prasad V. Katakam, Wiebke Arlt, Jochen Buck, Lonny R. Levin, Tony Hu, Jay Kolls, Charles F. Burant, Alejandra Tomas, Matthew J. Merrins, Debbie C. Thurmond, Ernesto Bernal-Mizrachi, David J. Hodson, and Franck Mauvais-Jarvis

Supplemental Information

Architecture of androgen receptor pathways amplifying glucagon-like peptide-1 insulinotropic action in male pancreatic β-cells

Weiwei Xu[†], Mirza Muhammad Fahd Qadir[†], Daniela Nasteska, Paula Mota de Sa, Caroline M. Gorvin, Manuel Blandino-Rosano, Charles R. Evans, Thuong Ho, Evgeniy Potapenko, Rajakrishnan Veluthakal, Fiona B. Ashford, Stavroula Bitsi, Jia Fan, Manika Bhondeley, Kejing Song, Venkata N Sure, Siva S.V.P. Sakamuri, Lina Schiffer, Wandy Beatty, Rachael Wyatt, Daniel E. Frigo, Xiaowen Liu, Prasad V Katakam, Wiebke Arlt, Jochen Buck, Lonny R. Levin, Tony Hu, Jay Kolls, Charles F. Burant, Alejandra Tomas, Matthew J. Merrins, Debbie Thurmond, Ernesto Bernal-Mizrachi, David J. Hodson, Franck Mauvais-Jarvis*

***Lead contact:** Email: fmauvais@tulane.edu

[†]The authors contributed equally to this work

Index:

1. Figure S1: Testosterone conversion to DHT via 5α-reductase is important for GSIS in mouse islets. Linagliptin improves glucose tolerance in βARKOMIP mice. Related to Figure 1.
2. Figure S2: Effect of DHT on GLP-1-, Exendin4- and FSK-stimulated cAMP production in 832/3 cells and on GLP-1-, GIP-, glucagon-, and FSK-stimulated GSIS in male mouse islets. Related to Figure 2.
3. Figure S3. Colocalization of AR and GLP-1R together and individually with endosomes. Related to Figure 2.
4. Figure S4. DHT does not alter GLP-1R membrane trafficking. Related to Figure 2.
5. Figure S5. DHT amplifies GLP-1 stimulated cAMP production at the plasma membrane and endosomes via sAC. Related to Figure 3-4.
6. Figure S6. QC metrics of scRNAseq in DHT-treated human islets. Related to Figure 5.
7. Figure S7. DHT alone or in the presence of GLP-1 promote AR dissociation from proteins favoring actin or microtubule polymerization. Related to Figure 6.
8. Figure S8. DHT-stimulated signaling network measured by RPPA. Related to Figure 7.
9. Table S1. Patient demographics Table
10. Table S2. Mass-to-charge (m/z) Transitions Used for the Quantification of Androgens

Figure S1: Related to Figure 1

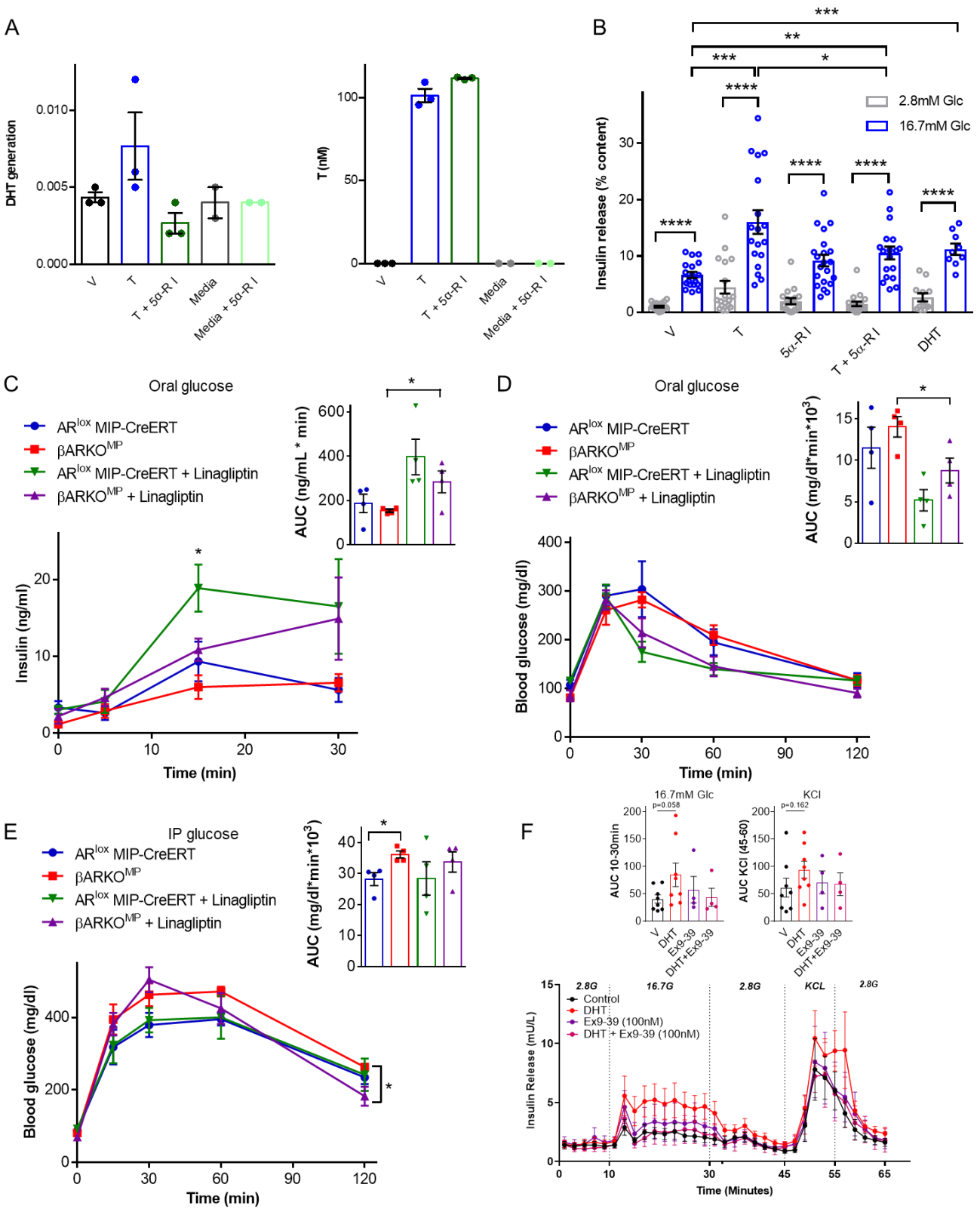

Figure S1: Testosterone conversion to DHT via 5α-reductase is important for GSIS in mouse islets. Linagliptin improves glucose tolerance in βARKO^{MIP} mice. Related to Figure 1.

(A) Steroid quantification by ultra-high-performance liquid-chromatography tandem mass spectrometry (UHPLC-MS/MS). Left: Generation of DHT from T (100nM) in male mouse islets is blocked by 5α-reductase inhibitors

(5α-RI), Finasteride (100nM) and Dutasteride (100nM). DHT concentrations were <LLOQ (0.24 nM) and hence no accurate quantification could be performed. DHT generation is shown as the ratio of the peak area of DHT and the peak area of its internal standard DHT-d3. Right: T recovery in the media. Values represent the mean ± SEM and scatter plot of technical triplicates for n=1 experiment (islets pooled from 10 male mice).

(B) GSIS was assessed in static incubation in cultured male islets from C57/BL6 mice treated with vehicle, T (10nM), finasteride (10nM) and dutasteride (10nM), for 40 minutes prior to measurement of insulin release by ELISA.

(C-E) Mice were exposed to a western diet since weaning and linagliptin was added to the diet (83mg/kg of diet) 4 weeks before investigations.

(C) Oral-GSIS (3 g/kg) with insulin area under the curve (AUC) was performed at the indicated mice with and without linagliptin treatment. In response to an O-GTT, linagliptin improved GSIS in both control and βARKO^{MIP} mice compared to those without linagliptin treatment. Mice were studied at 40-45 weeks of age.

(D) Oral-GTT (2 g/kg) with glucose AUC was performed at the indicated mice with and without linagliptin treatment. In response to an O-GTT, linagliptin improved glucose tolerance in both control and βARKO^{MIP} mice compared to those without linagliptin treatment

(E) IP-GTT (2 g/kg) with glucose AUC was performed at the indicated mice with and without linagliptin treatment. During an IP-GTT, linagliptin-treated βARKO^{MIP} mice were no longer glucose intolerant compared to linagliptin-treated controls. At 2h into the IP-GTT, blood glucose was significantly lower in linagliptin-treated βARKO^{MIP} mice compared to untreated βARKO^{MIP} mice.

(F) Dynamic insulin secretion measured via perifusion in male human islets challenged with 2.8mM glucose, 16.7mM glucose and KCl 30mM + 16.7mM glucose. Islets were cultured overnight in vehicle or DHT (10nM). During perifusion islet were treated with vehicle, DHT, Exendin9-39 (100nM) or DHT + Exendin9-39. Secretion values not normalized to baseline but to total insulin content to adjust for beta cell number.

Values represent the mean ± SE of n= 3-5 mice/group. * P < 0.05, ** P < 0.01, *** P < 0.001, **** P < 0.0001.

Figure S2: Related to Figure 2

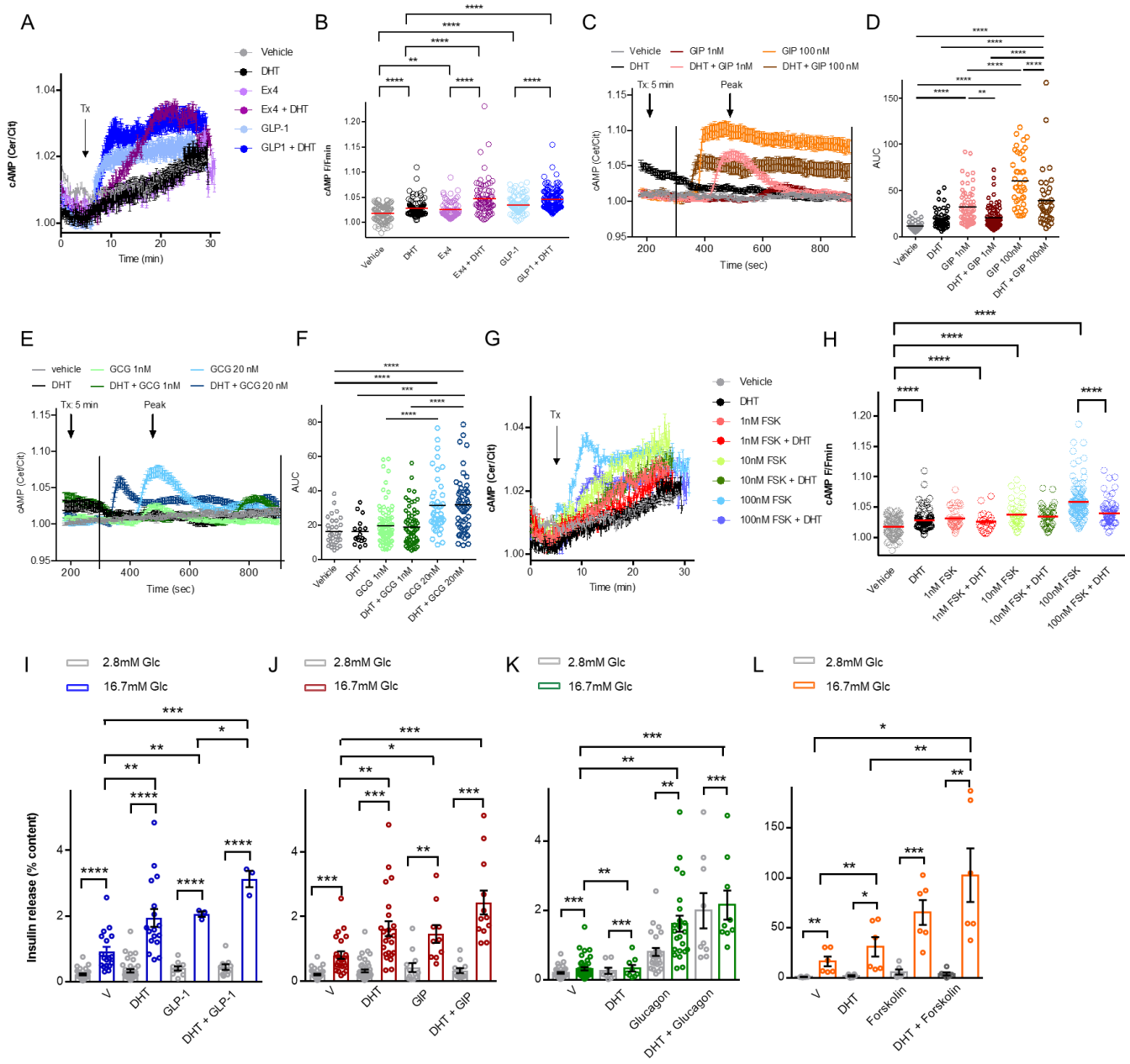

Figure S2. Effect of DHT on GLP-1-, Exendin4- and FSK-stimulated cAMP production in 832/3 cells and on GLP-1-, GIP-, glucagon-, and FSK-stimulated GSIS in male mouse islets. Related to Figure 2.

(A) 832/3 cells were infected with adenovirus harboring the FRET Epac2 camps probe and treated with DHT (10nM), GLP-1 (10nM), and exendin4 (Ex4, 10nM) starting at the indicated time (Tx arrow, 5 min). cAMP production was monitored in real-time from live cells.

(B) Summary graph showing amplitude of cAMP responses from **(A)**.

(C) 832/3 cells were infected with adenovirus harboring the FRET Epac2 camps probe and treated with DHT (10nM) and GCG (1nM, 20nM) starting at the indicated time (Tx arrow, 5 min). cAMP production was monitored in real-time from live cells.

(D) Summary graph showing amplitude of cAMP responses from **(C)**.

(E) 832/3 cells were infected with adenovirus harboring the FRET Epac2 camps probe and treated with DHT (10nM) and GIP (1nM, 100nM) starting at the indicated time (Tx arrow, 5 min). cAMP production was monitored in real-time from live cells.

(F) Summary graph showing amplitude of cAMP responses from **(E)**.

(G) 832/3 cells were infected with adenovirus harboring the FRET Epac2 camps probe and treated with DHT (10nM) and forskolin (FSK) at the indicated concentration starting at the indicated time (Tx arrow, 5 min). cAMP production was monitored in real-time from live cells.

(H) Summary graph showing amplitude of cAMP responses from **(G)**.

Note that vehicle/DHT values in **(A)** and **(G)** are identical, since the Ex4, GLP1 and FSK states were run in parallel with the same controls but are shown on separate graphs for clarity. GSIS was assessed in static incubation in cultured male islets from C57/BL6 mice.

(**I-L**) Cultured islets were treated with vehicle, DHT (10nM), and **(I)** GLP-1 (10nM), **(J)** GIP (100nM), **(K)** glucagon (20nM) and **(L)** forskolin (100nM) for 40 minutes prior to measurement of insulin release by ELISA. Values represent the mean ± SE of n= 2-4 mice/group measured in triplicate. $^{*}P < 0.05$, $^{**}P < 0.01$, $^{***}P < 0.001$, $^{****}P < 0.0001$

Figure S3: Related to Figure 2

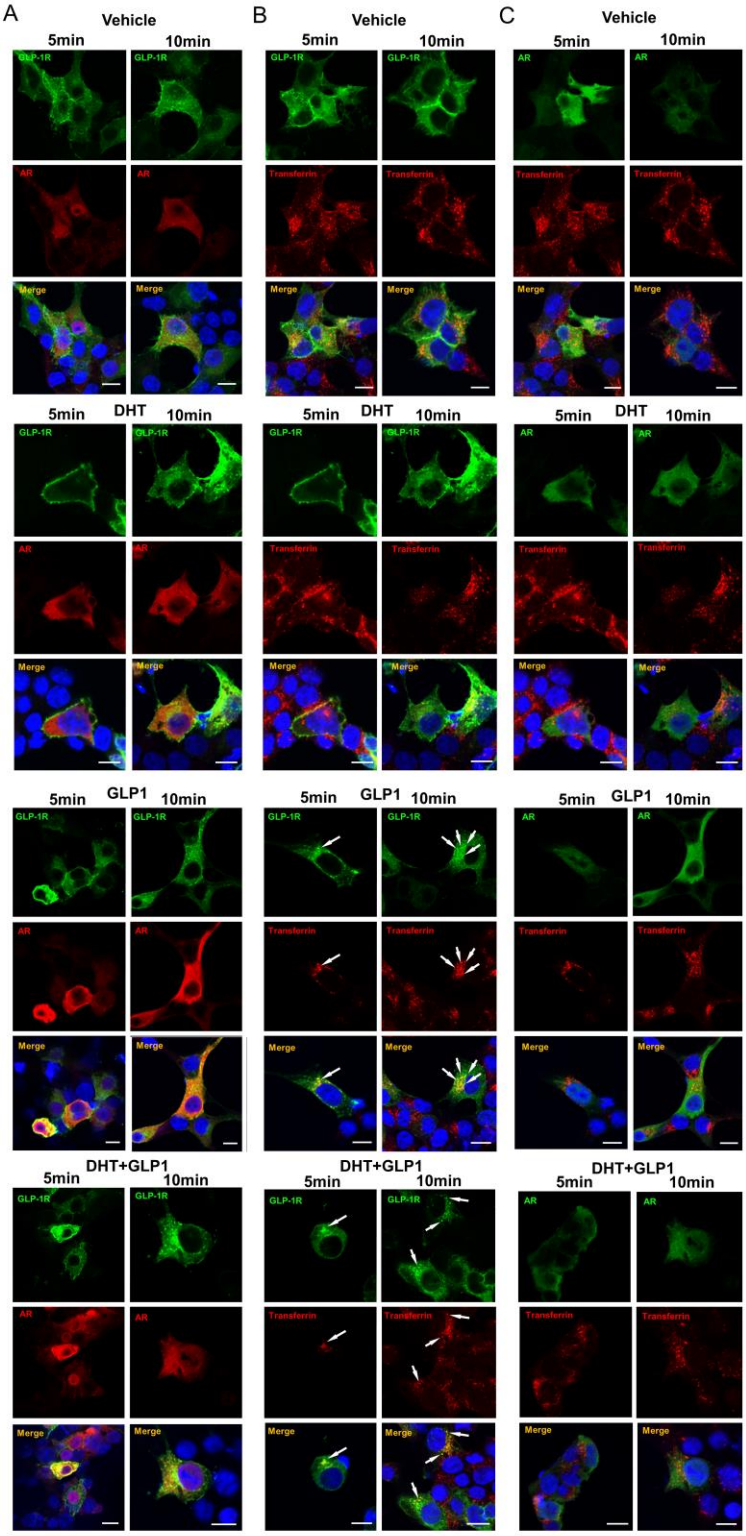

Figure S3. Colocalization of AR and GLP-1R together and individually with endosomes. Related to Figure 2.

(A) INS1 832/3 cells were transfected with GLP-1R-GFP (green) and FLAG-AR (red) and treated with vehicle, DHT (10nM), GLP-1 (10nM) and DHT + GLP-1 for 5- or 10-min. Receptors localization was assessed by immunofluorescence. Images were captured by confocal microscopy. Representative pictures are shown.

(B) INS1 832/3 cells were transfected with GLP-1R-GFP (green) and transferrin-555 (red) and treated with vehicle, DHT (10nM), GLP-1 (10nM) and DHT + GLP-1 for 5 or 10 min. Cells were treated with transferrin-555 to label the endosomal pathway. GLP-1R colocalization with endosomes was assessed by immunofluorescence and is shown with white arrows. Images were captured by confocal microscopy. Representative pictures are shown.

(C) INS1 832/3 cells were transfected with FLAG-AR (green) and transferrin-555 (red) and treated with vehicle, DHT (10nM), GLP-1 (10nM) and DHT + GLP-1 for 5 or 10 min. Cells were treated with transferrin-555 to label the endosomal pathway. AR colocalization with endosomes was assessed by immunofluorescence and AR does not localize in endosomes. Images were captured by confocal microscopy. Representative pictures are shown. Scale bars: 5µm.

Figure S4: Related to Figure 2

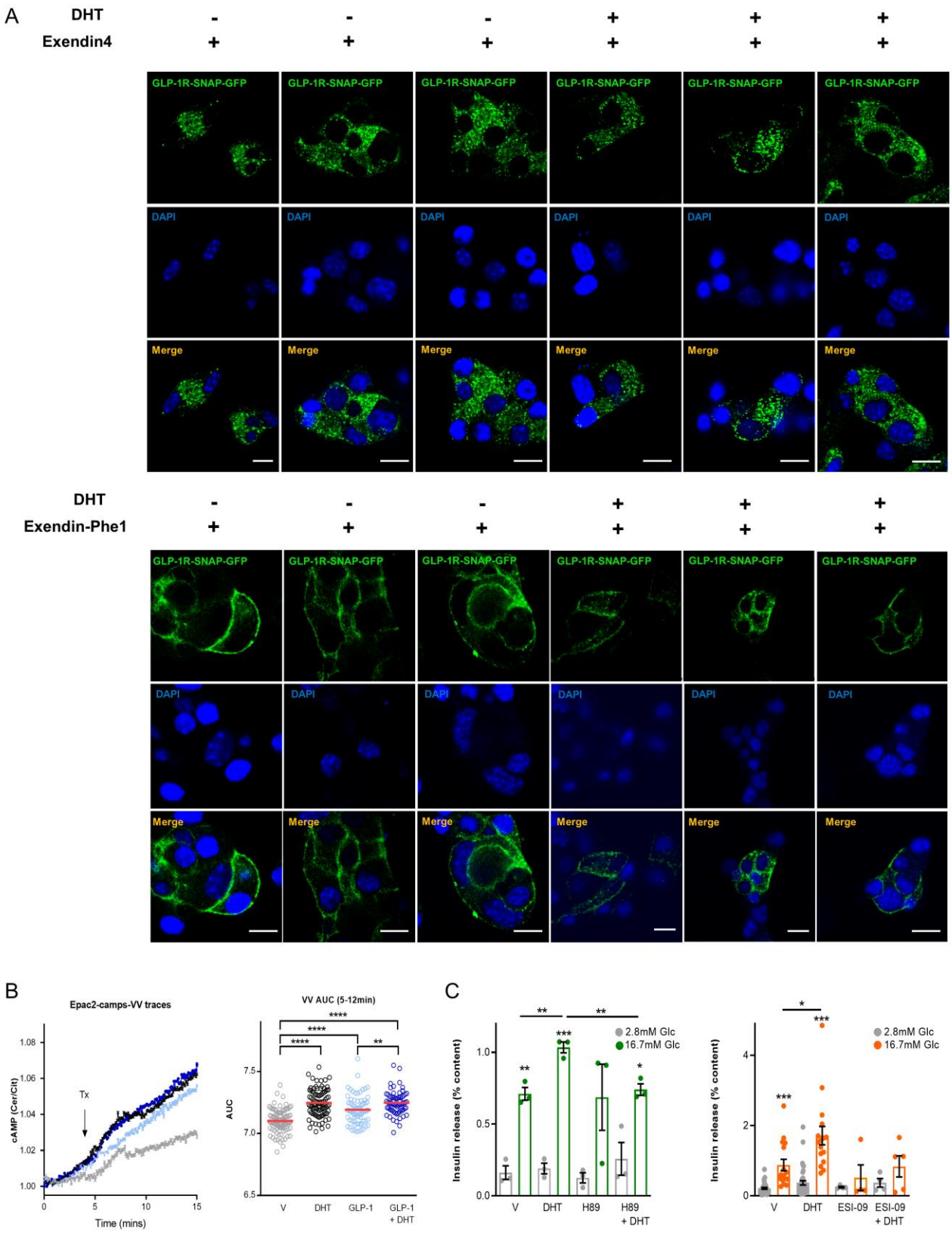

Figure S4. DHT does not alter GLP-1R membrane trafficking. Related to Figure 2.

(A) MIN6B1 cells stably expressing human SNAP-GLP-1R cells were labelled with SNAP-Surface 549 to label surface receptors and treated for 30 min with 100 nM Exendin-4 or the biased agonist Exendin-Phe1 in the

presence or absence of 10 nM DHT. Images were captured by confocal microscopy. Representative pictures are shown. Scale bars: 5µm.

(B) Left: 832/3 cells were transfected with organelle-targeted cAMP FRET biosensors and treated with DHT (10nM), GLP-1 (10nM) and DHT + GLP-1. Epac2-camps plasmids targeted to the cytoplasm (Epac2-camps-VV traces) (n = 4 independent replicates, 55-103 cells); right: AUC of the cAMP peak between 5 and 12 min.

(C) GSIS was measured in static incubation in wild-type male mouse (n= 2 mice/group measured in triplicate) treated with vehicle, DHT (10nM) for 40 minutes in the presence of absence of H89 (10uM) or ESI-09 (10uM).

Figure S5: Related to Figure 3-4

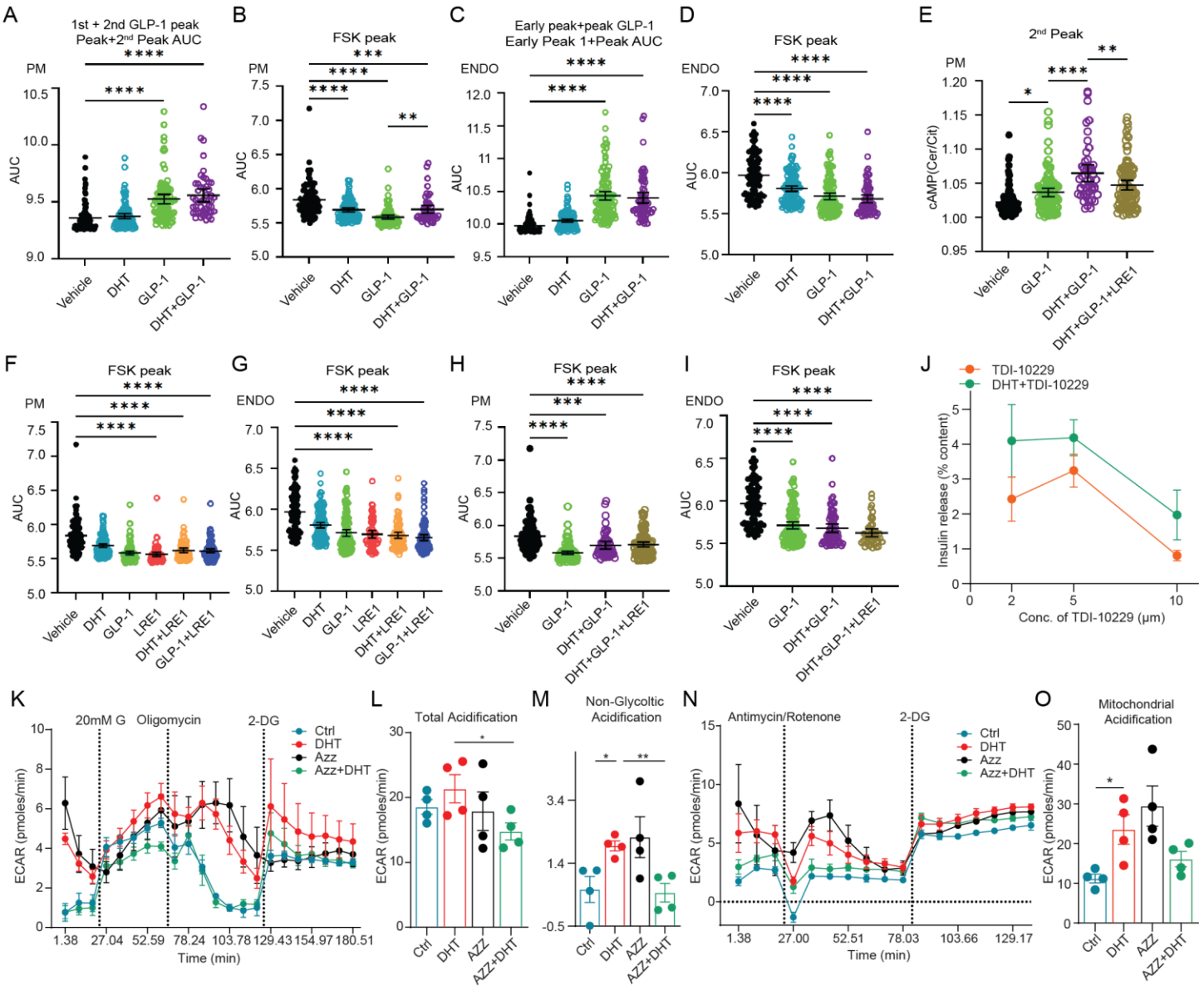

Figure S5. DHT amplifies GLP-1 stimulated cAMP production at the plasma membrane and endosomes via sAC. Related to Figure 3-4.

(A-H) 832/3 cells were transfected with Epac2-camps plasmids targeted to the plasma membrane (Epac2-vvPM) or the endosomes (Epac2-camps-vv-Endo) and treated with DHT (10nM), GLP-1 (10nM) and DHT + GLP-1 in the presence of absence of sAC inhibitor LRE-1 (10uM). Forskolin (FSK) was added at 15min. Data represent n = 4 independent replicates of 55-103 cells.

(A) Area under the curve (AUC) of 1st + 2nd GLP-1-stimulated peak of cAMP at the PM from **(F3A)**

(B) AUC of FSK-stimulated peak of cAMP at PM from **(F3A)**.

(C) AUC of GLP-1-stimulated early peak + peak of cAMP at ENDO from **(F3C).**

(D) AUC of FSK-stimulated peak of cAMP at ENDO **(F3C)**.

(E) 2nd peak of cAMP at PM from **(F3I)**.

(F) AUC of FSK peak of cAMP at PM from **(F3E)**.

(G-I) AUC of FSK peaks of cAMP at ENDO and PM from **(F3G, F3I and F3K)**

(J) Dose response curve showing the GSIS of human islets treated with the sAC inhibitor TDI-10229 at varying concentrations.

(K-O) Extracellular acidification rate (ECAR) was measured in a seahorse analyzer during **(K-M)** a glycolytic stress test using 2-DG and **(N-O)** a mitochondrial test using antimycinA/rotenone at the indicated times. 20 islets were loaded in a 4 separate wells from 1 male human donor. **(A-K)** Data represent 10 IEQ/condition, measured in triplicate of n=3-4 donors. **(A-O)** Values represent the mean ± SE. * $P < 0.05$, ** $P < 0.01$, *** $P < 0.001$, **** $P < 0.0001$.

Figure S6: Related to Figure 5.

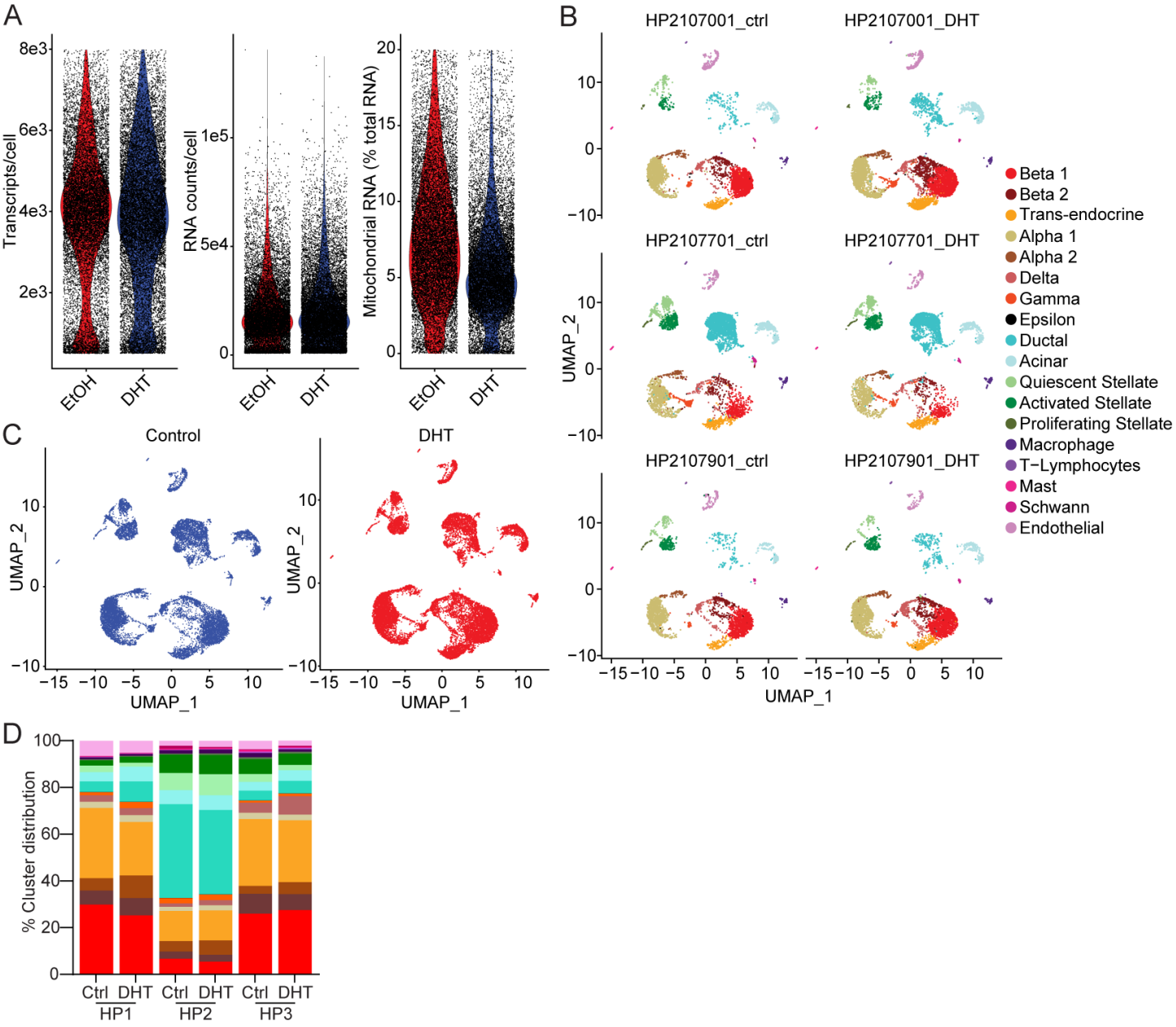

Figure S6. QC metrics of scRNAseq in DHT-treated human islets. Related to Figure 5.

(A) Violin plots showing the distribution of transcripts, RNA molecule counts and mitochondrial RNA percentage in each cell and across the data.

(B) UMAP plots showing the distribution of cell clusters across all 6 individuals sets of data. Each map shows integrated data for a specific donor or treatment.

(C) UMAP plots showing the distribution of integrated cells in control (blue) and DHT treated (red) islet cells. Results show optimal integration and distribution of cells across all clusters.

(D) Plot showing the contribution of each cluster as shown in **(B).**

Figure S7: Related to Figure 6

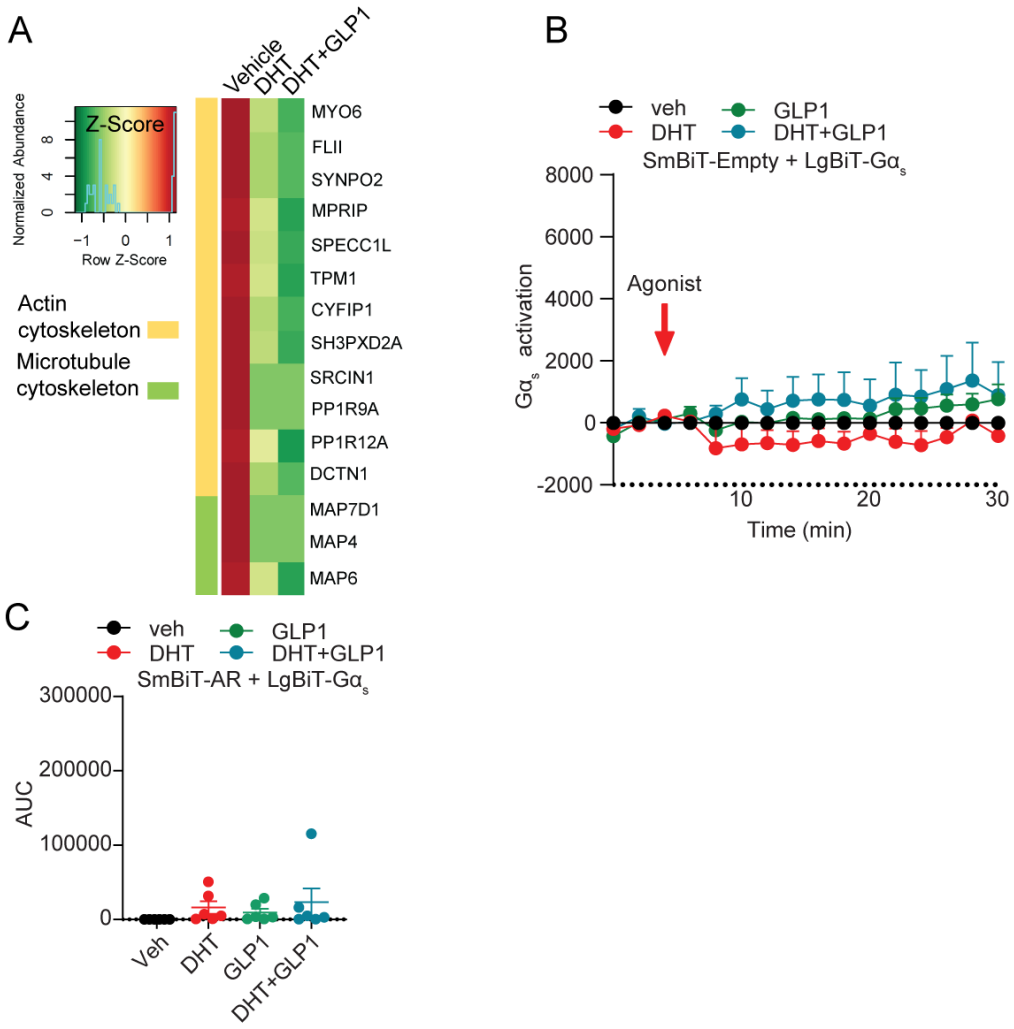

Figure S7. DHT alone or in the presence of GLP-1 promote AR dissociation from proteins favoring actin or microtubule polymerization. Related to Figure 6.

(A) IP-based proteomics analysis was performed in INS1 832/3 cells. Heatmap constructed by integrating the GO analysis with the Ingenuity Pathway Analysis (IPA) showing AR dissociation from proteins favoring actin or microtubule polymerization.

(B) INS1 832/3 cells where transfected with SmBiT-Empty control and LgBiT-$G\alpha_s$ and treated with DHT (10nM) or GLP-1 (10nM) for the indicated time. Line graph shows $G\alpha_s$ recruitment to empty control.

(C) AUC for **(B)**.

Figure S8: Related to Figure 7

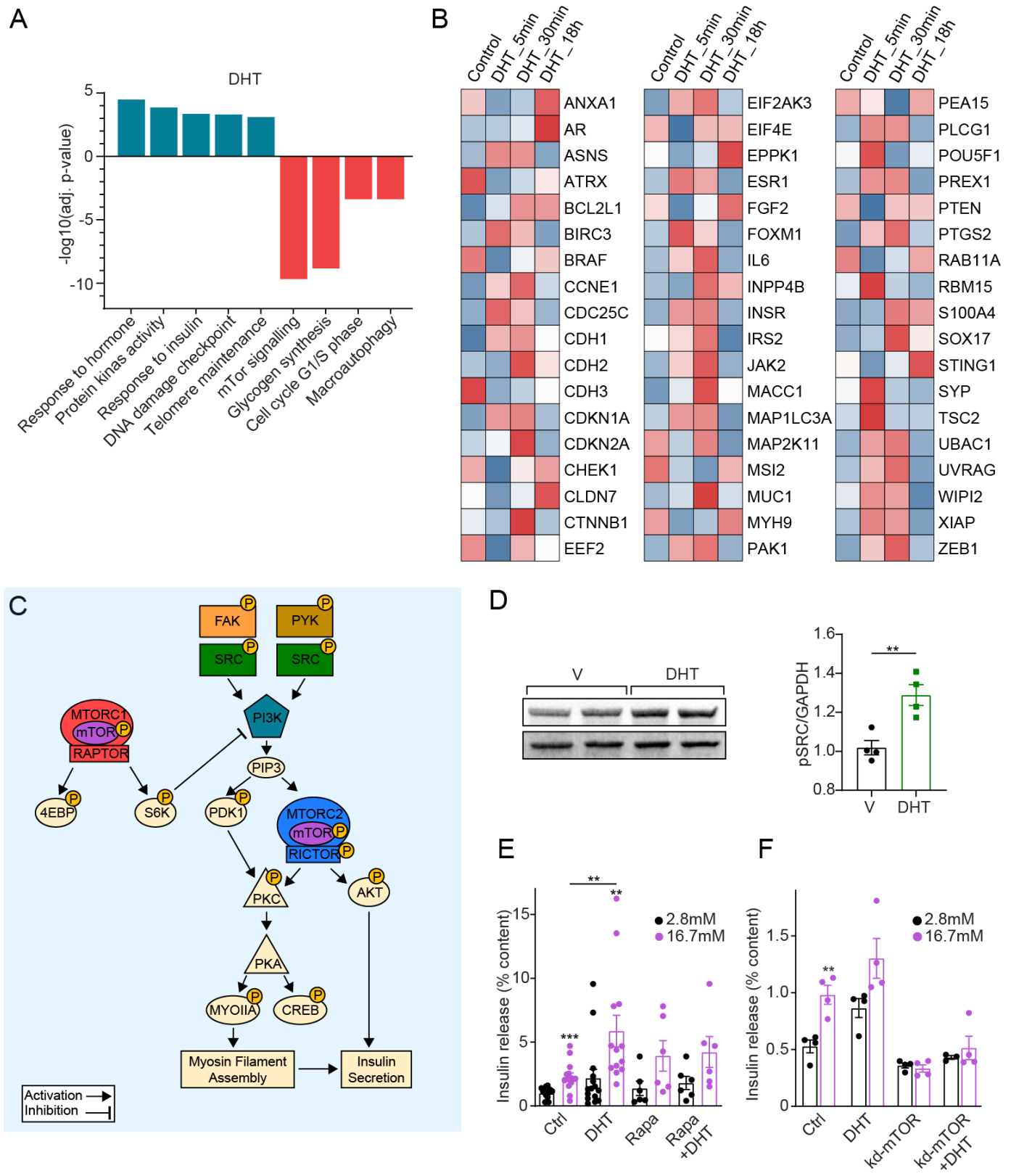

Figure S8. DHT-stimulated signaling network measured by RPPA. Related to Figure 7.

(A) Barplot showing gene ontology (GO) enrichment analysis of proteins expression following 18h of DHT (10nM) treatment and focused on the “Biological Process” domain.

(B) Heatmap of selected proteins in islets at 5min, 30min and 18hrs of DHT (10nM) treatment compared to controls.

(C) Schematic representation of signaling cascade from selected phosphoproteins identified in the RPPA and involved in insulin secretion.

(D) Enhancement of phosphorylated SRC expression following DHT (10nM) treatment.

(E and F) GSIS was measured in static incubation in islets treated with vehicle or DHT (10nM) for 40 minutes.

(E) mTOR inhibitor rapamycin (27.4nM) (n=2 human cadaveric donors measured in triplicate, n=10 IEQ per replicate)

(F) Male control and littermate (kd)-mTOR mice (n=4 mice, with each condition measured in triplicate, n=10 islets per replicate).

Table S1: **Human Islet Donor Profile. Related to Figure 1-7.**

Sample ID	Diabetes Status	BMI	Age (Years)	Sex	Race	Figures
SAMN10357324	Non-diabetic	40	44	M	White	F2R-S, SF8E
SAMN10374868	Non-diabetic	32.4	58	M	N/A	F2R-S, SF8E
HP-20152-01	Non-diabetic	20.2	48	M	African American	F1L
HP-20206-01	Non-diabetic	31.9	22	M	Hispanic	F3M
SAMN15656747	Non-diabetic	33.6	24	M	N/A	F3M
HP-20215-01	Non-diabetic	32.8	56	M	Hispanic	F3M, F6L
HP-20220-01	Non-diabetic	29.3	60	M	Asian	F1L, F3M
HP-20245-01	Non-diabetic	20.0	24	M	Hispanic	F1L, F3M, F6L
HP-20262-01	Non-diabetic	24.4	67	M	Asian	F1L, F4Q, F7A, SF8A-B
HP-20276-01	Non-diabetic	31.3	25	M	Caucasian	F1L
HP-20281-01	Non-diabetic	25.8	55	M	Caucasian	F1L, F4Q, F7A, SF8A-B
SAMN16452455	Non-diabetic	31.1	39	M	Caucasian	F1L
HP-20314-01	Non-diabetic	28.0	37	M	African American	F4Q, F7A, SF8A-B
HP-20318-01	Non-diabetic	22.1	48	M	Native American	F1L, F7I-J
HP-21006-01	Non-diabetic	29.6	54	M	Asian	F7H
HP-21013-01	Non-diabetic	10	20	M	African American	F7H, F7I-J
HP-21024-01	Non-diabetic	20.3	51	M	Caucasian	F7H, F7I-J
HP-21028-01	Non-diabetic	29.3	41	M	Hispanic	F7H
HP-21045-01	Non-diabetic	23.6	31	M	Hispanic	F7H
HP-21047-01	Non-diabetic	24.3	56	M	Hispanic	F7E
HP-21070-01	Non-diabetic	22.7	39	M	Caucasian	F5A-M, F7E
HP-21077-01	Non-diabetic	28.7	44	M	Asian	F5A-M
HP-21079-01	Non-diabetic	22.6	59	M	Caucasian	F5A-M, F7E
HP-21132-01	Non-diabetic	26.6	31	M	Caucasian	F3N, F7F
HP-21141-01	Non-diabetic	21.3	55	M	Caucasian	F3N, F7F
HP-21146-01	Non-diabetic	23.1	19	M	Caucasian	F3N, F7F
HP-21148-01	Non-diabetic	27.6	39	M	Caucasian	F3N
HP-21227-01	Non-diabetic	31.8	59	M	Caucasian	F4R-S
SAMN218554451	Non-diabetic	35.1	55	M	Caucasian	F4R-S, F4A-C, F7B, FS5J
HP-21272-01	Non-diabetic	29.0	39	M	Caucasian	F4R-S, F4A-C, F7B, FS5J
HP-21287-01	Non-diabetic	27.6	44	M	Caucasian	F4A-C, F7B, FS5J
HP-21302-01	Non-diabetic	20.4	30	M	Hispanic	F3O, F4A-C, F6L, F7C,D, FS5J
HP-21324-01	Non-diabetic	25.7	44	M	Hispanic	F3O, F4A-C, F6L, F7C,D, FS5J
HP-21337-01	Non-diabetic	30.3	26	M	Hispanic	F3O, F4A-C, F6L, F7C,D, FS5J
HP-22030-01	Non-diabetic	25.6	36	M	Asian	F4A-C
SAMN30927409	Non-diabetic	36.3	50	M	N/A	F7L-O
SAMN30631345	Non-diabetic	21.5	16	M	N/A	F7L-O
SAMN28569417	Non-diabetic	40.7	64	M	N/A	F7L-O
SAMN27619977	Non-diabetic	31.3	37	M	N/A	F7L-O
SAMN27521605	Non-diabetic	34.9	31	M	N/A	F7L-O
HP-23052-01	Non-diabetic	22.1	63	M	Caucasian	SF5K-O

Table S2. Mass-to-charge (m/z) Transitions Used for the Quantification of Androgens. Related to Figure 1.

Steroid	***m/z* transitions Quantifier Qualifier**
Analytes	
Testosterone	289.1 > 96.9 289.1 > 109.0
Dihydrotestosterone (DHT)	291.3 > 255.1 291.1 > 159.0
Internal standards	
Testosterone-D3	292.1 > 96.9
DHT-D3	294.1 > 258.1